Proceedings of IMECE2002
ASME International Mechanical Engineering Congress & Exposition
November 17-22, 2002, New Orleans, Louisiana

IMECE2002-33598

CONFIGURATION-SPACE SEARCHING AND OPTIMIZING TOOL ORIENTATIONS FOR 5-AXIS MACHINING

Cha-Soo Jun
Division of Industrial and Systems Engineering, Gyeongsang National University, Jinju, 660-701, South Korea

Yuan-Shin Lee*
Department of Industrial Engineering, North Carolina State University, Raleigh, NC 27695-7906, U.S.A.

Kyungduck Cha
School of Industrial and Systems Engineering, Georgia Institute of Technology, Atlanta, GA, U.S.A

*: To whom all the correspondence should be addressed

ABSTRACT

This paper presents a methodology and algorithms of optimizing and smoothing the tool orientation control for 5-axis sculptured surface machining. A searching method in the machining *configuration space* (C-space) is proposed to find the optimal tool orientation by considering the local gouging, rear gouging and global tool collision in machining. Based on the machined surface error analysis, a boundary search method is developed first to find a set of feasible tool orientations in the C-space to eliminate gouging and collision. By using the minimum cusp height as the objective function, we first determine the locally optimal tool orientation in the C-space to minimize the machined surface error. Considering the adjacent part geometry and the alternative feasible tool orientations in the C-space, tool orientations are then globally optimized and smoothed to minimize the dramatic change of tool orientation during machining. The developed method can be used to automate the planning and programming of tool path generation for high performance 5-axis sculptured surface machining. Computer implementation and examples are also provided in the paper.

Key Words: 5-axis CNC machine, sculptured surface machining, optimal tool orientation, configuration space search, edge detection algorithm, CAD/CAM

INTRODUCTION

Five-axis NC machines are widely used in machining of sculptured surfaces such as aircraft parts, turbine blades, impellers, propellers, 3D cams, molds and dies. Since 5-axis machines have two more degrees of freedom than traditional 3-axis machines, 5-axis machining offers many advantages over 3-axis machining, including better tool accessibility, faster material removal rates and improved surface finish [Choi 98, Jerard 91]. To make the best use of 5-axis machines, however, we have to solve more complicated interference (gouging and collision) problems and to determine the optimal tool orientations for complex surface machining.

Gouging and tool collision are the main problems in machining sculptured surfaces [Lee 95, Suresh 94]. As shown in Figure 1, the cutter interference in 5-axis machining can be classified into three types, *local gouging*, *rear gouging* and *global collision*, according to the interference checking area [Deng 96, Ray 92]. Local gouging refers to the removal of the excess material in the vicinity of the cutter contact (CC) point due to the mismatch in curvatures between the tool swept surface and the part surface at the CC point. Several researchers have developed techniques to detect and avoid local gouging by comparing the effective cutting curvature of the tool swept surface to the normal curvature of the part surface at the CC point [Kruth 99, Lee 95, Rao 00]. As shown in Figure 1, rear gouging exists when the interference occurs between the bottom of the endmill cutter and the part surface. Global collision is the interference of the cylindrical part of the tool or tool holder and the part surface, including fixtures [Choi 98, Lo 99, Lee 95, Elber 99]. Choi *et al*.[1993] proposed a scheme that searched the feasible regions considering the special case of marine propeller machining and minimized cusp heights derived analytically. As for the optimal tool orientation or good positioning issues, many studies are using concepts of differential geometry such as local curvature properties [Rao 00, Jensen 93, Lee 97b, Kruth 99]. The curvature-matching schemes have some difficulties handling rear gouge and global collision in a unified manner [Choi 98].

Currently, the available commercial CAD/CAM software for 5-axis machining still lacks flexibility when specifying the tool orientation and tool path distribution for complex surface machining [Choi 93, Kim 95, Lee 97a]. Traditionally the orientation of the endmill has remained fixed during machining. For example, the tool orientation is set to an angle that ranges from

3^o to 10^o off the principal surface normal during tool motion. Although this approach is demonstrably more efficient than 3-axis sphere-endmill machining [Vickers 89], gouging and tool collision problems remain, and scallops left on surface need manual grinding and reworking of the machined surface [Lee 98a, Li 94, Marciniak 87]. Although inclining the cutter generally prevents its trailing edge from dragging across the surface, this fixed-orientation method suffers some machining efficiency and gouging problems. These problems are exacerbated when the sculptured surfaces become more complex. The traditional fixed-orientation practice cannot effectively prevent gouging problems during tool path planning for complex surface machining.

Machined surface errors resulting from tool path generation are typically determined using *posterior* tool path checking and graphic visualization techniques [Choi 98, Elber 99, Morishige 99]. Although these checking techniques have proven useful in identifying the tool path errors after actual machining, the problems of generating an error-free tool path remain. Currently, intensive user interaction is still needed while using CAD/CAM software to generate NC part programs for sculptured surface machining, which requires considerable checking, verification, and reworking [Kim 95, Lee 97b, Rao 00]. These problems must be solved so that the full advantages of 5-axis machining can be exploited more widely.

In this paper, we focus on the investigation of a searching method in the machining *configuration space* (C-space) based on the different machining constraints and a global smoothing method to find the optimal tool orientation for 5-axis machining. We start with a tool path given as a sequence of cutter contact points. We will find at each cutter contact point the orientation of the tool that minimizes cusp height while avoiding gouging and interference. Our method works by considering the parameter space for tool orientations, and finding the region(s) of orientations that avoid gouging and interference. We then find the point within each region that results in minimum cusp height. Key to our method is determining cusp height and detecting gouging/ interference. We discuss the former in Sections 3 to 4 and the latter in Section 5. Section 6 presents a complete algorithm of finding the global optimal tool orientations for 5-axis machining, followed by the examples and the concluding remarks.

2. TOOL ORIENTATION CONTROL IN 5-AXIS MACHINING

In this section, the coordinate systems of 5-axis machining and the cusp height analysis are first introduced and they will be used later in the algorithms for gouging/interference detection. In Figure 2, the three unit vectors and a cutter contact (CC) point $\mathbf{r}_c$ are used to construct a local orthogonal coordinate frame ($\mathbf{f}$, $\mathbf{t}$, $\mathbf{n}$, $\mathbf{r}_c$), called the CC-coordinate system: $\mathbf{f}$ denotes the unit vector for the cutter feed direction which is tangent to the surface; $\mathbf{n}$ denotes the unit normal vector of the surface; $\mathbf{t}$ is a unit tangent vector of the surface defined as $\mathbf{t} = \mathbf{n} \times \mathbf{f}$ [Choi 98]. It is convenient to define a tool axis vector $\mathbf{u}$ of a flat-endmill in the CC-coordinate system. As illustrated in Figure 2, the angle between tool axis vector $\mathbf{u}$ and normal vector $\mathbf{n}$ is called the *tilt angle* α, and if the tool is rotated around the normal vector $\mathbf{n}$, the rotate angle is called the *yaw angle* β. In this paper, a *tool orientation* is defined by (α, β).

To avoid gouging in sculptured surface machining, cutters can be tilted and rotated along the two additional axes to better fit the cutting shapes onto the curved surfaces [Chiou 99, Lo 99, Rao 00]. Depicted in Figure 3(a) is the bottom face of a flat-endmill viewed from the cutter feed vector $\mathbf{f}$. The projected bottom face of the tool onto the **t-n** plane becomes an ellipse, which is called the *effective cutting ellipse E* [Choi 98, Lee 98b]. As discussed earlier in [Chiou 99, Choi 93, Kim 94, Lee 95], the cutting ellipse E is dependent on the tool orientation (α, β) and it is denoted as $E(\alpha, \beta)$. By changing the angles (α, β), the cutter can be more closely fitted to the surface, as shown in Figures 3(b) and 3(c). Notice that, in Figure 3(a), the major radius of the cutting ellipse $E(\alpha, \beta)$ is equal to the cutter radius r. Let θ be the angle between the major axis of the ellipse $E(\alpha, \beta)$ and the y axis. The θ and the minor radius a of the cutting ellipse $E(\alpha, \beta)$ are given as follows (also in Figure 3):

$$a = | r \sin\alpha \cos\beta | \qquad (1)$$

$$\theta = \tan^{-1}(-\tan\alpha \sin\beta) \qquad (2)$$

Figures 3(b) and 3(c) illustrate the effects of the cutting ellipse $E(\alpha, \beta)$ by changing the tilt (α) and yaw (β) angles. Figure 3(b) shows the changes of the cutting ellipses $E(\alpha, \beta)$ according to the tilt angle α when the yaw angle $\beta = 0$. The yaw angle β is related to the symmetry of the cutting ellipse $E(\alpha, \beta)$ as shown in Figure 3(c). The yaw angle has traditionally been fixed to zero in most of the previous methods, such as curvature matched machining methods [Marciniak 87].

Figure 4 shows a machined surface that is determined by the silhouette of the cutter, including the instantaneous cutter cylinder and the effective cutting shape $E(\alpha, \beta)$ projected onto a 2D plane perpendicular to the cutting direction [Cho 93, Lee 95]. As shown in Figure 4, the cutting ellipse shape is a function of the tool orientation (α, β), and it can be used for finding the machined surface errors [Choi 93, Kim 94, Lee 95]. Since the exact cusp heights for 5-axis milling are determined by cutter movement along two adjacent tool paths, they can be computed only from an extensive cutting simulation and surface evaluation, as shown in Figure 4. In an optimization process, however, it is almost impossible to consider simultaneously the tool orientations at all the CC points to calculate exact cusp heights h [Choi 98]. In previous research, the cusp height h is calculated after each cutting ellipse E is approximated by a circular arc whose radius is assigned to be the radius of curvature of the ellipse at its CC point [Kim 94, Li 94]. In another method [Choi 93], the cusp height is approximated by the identical ellipses. Both methods for cusp height approximation are simple to calculate but cannot reflect the effects of yaw angle.

To simplify the computation, in this paper, we use a method for quick computing of the cusp heights h [Jun 02]. As shown in Figure 4(b), the approximate cusp height h is the normal distance from the position $\mathbf{p}_s$ on the surface in the middle between two adjacent tool paths. As shown in Figures 4(b) and 4(c), the cusp height h can be found as follows:

$$h = | \mathrm{p_i} - \mathbf{p}_s |$$
$$\mathbf{p}_i = L(\mathbf{p}_s, \mathbf{n}_s) \cap [E(\alpha, \beta) + Cutter\_Shaft\_Silhouette] \qquad (3)$$

where $\mathbf{p}_S$ is a point on the part surface, $\mathbf{n}_S$ is the surface normal at $\mathbf{p}_S$, and $\mathbf{p}_I$ is the intersection of the normal line $L(\mathbf{p}_S, \mathbf{n}_S)$ and the cutting ellipse $E(\alpha, \beta)$ plus the cutter shaft silhouette located at surface point $\mathbf{p}_S$. If neither the cutting ellipse nor the cylinder profile is intersected with the line $(\mathbf{p}_s, \mathbf{n}_s)$, a preset value (i.e., machining thickness) is assigned as the cusp height, as shown in Figure 4(c). Details of calculating the cusp height h as shown in Equation (3) can be found in [Jun 02]. The technique of quick-estimation of the cusp height (h) is used to construct the machining configuration space for planning and decision, as discussed later in Section 4.

3. MACHINED SURFACE ERRORS ANALYSIS FOR 5-AXIS MACHINING

This section presents the formulation of machined surface analysis during 5-axis simultaneous tool motions, which will be used later in the algorithms of finding the optimal tool orientations.

Due to the two additional rotation axes in 5-axis machining, both the cutter location (CL) and the tool orientation need to be determined in cutter path generation. In 5-axis machining, because of the complex tool motion during machining, it is not easy to determine the cutter location (CL) and tool orientation data for complex surface machining with gouging avoidance [Jerard 91, Lee 97a]. In this paper, we focus on the investigation of finding the admissible tool orientation for both gouging avoidance and global collision avoidance in 5-axis machining.

In 5-axis machining, to avoid gouging around the cutter contact (CC) point, the effective cutting shapes $E(\alpha, \beta)$ of the cutter need to fit into the local surface shapes, as shown earlier in Figure 3. As shown in Figure 4(b), h_{left} and h_{right} are the adjacent cusp heights at the cutter contact point, and they can be found by using Equation (3). Given a cutter Ψ with a radius r and a set of pre-defined cutter contact paths $\{CC_i\}$, the effective cutting ellipse E^{Ψ} of the tool motions can be found as follows:

$$E^{\Psi} = E^{\Psi}(\Psi_r, \{CC_i\}) = \bigcup_{i=0}^{n} E^{\Psi}_i(\Psi_r, \{CC_i\}) \qquad (4)$$

where $\{CC_i\}_{i=0,..,n}$ are the pre-defined cutter contact paths. To find the machined surface errors, the cusp heights $h_{i,left}$ and $h_{i,right}$ of a set of given tool path $\{CC_i\}$ are calculated. In the earlier work presented in [Chiou 99], the intermediate machined surface can be defined as the *conjugate geometry* of the shape generation function of the cutter and the part surface. Given a cutter Ψ and a pre-defined tool path $\{CC_i\}$, the machined part surface G^{Ψ}_i is the conjugate geometry defined by the swept envelope E^{Ψ}, and it can represented as follows:

$$G^{\Psi}_{i+1} = G^{\Psi}_i - E^{\Psi}_i(\Psi_r, \{CC_i\}) \qquad (5)$$

where G^{Ψ}_i is the current machined surface geometry G-buffer model at i (and $i \in [0, n]$) and E^{Ψ}_i is the effective cutting ellipse. The machined surface errors can be analyzed by using the constructed G-buffer models and the designed part surface. Given a cutter Ψ and a pre-defined tool path $\{CC_i\}$, the machined surface error δ^{Ψ} can be found as follows:

$$\delta^{\Psi} = \Delta G^{\Psi}_{n+1} = G^{\Psi}_{n+1} - PS \qquad (6)$$

where PS is the designed part surface and G^{Ψ}_{n+1} is the constructed G-buffer model of part surface updated by all the swept envelope E^{Ψ}_i as defined in Equation (5). For manufacturing, the machined surface error δ^{Ψ} needs to be controlled within a given tolerance τ (i.e., $|\delta^{\Psi}| \le \tau$), shown as follows:

$$|\delta^{\Psi}| = |\Delta G^{\Psi}_{t=t_n}| = \text{Max}\{h^{\Psi}_{i,left}, h^{\Psi}_{i,right}\}$$
$$i=0,\ldots,n \le \tau \qquad (7)$$

where δ^{Ψ} is the maximum machined surface errors, $h^{\Psi}_{i,left}$ and $h^{\Psi}_{i,right}$ are the correspondent left and right cusp heights defined earlier, and τ is the allowable surface tolerance. The machined surface errors δ^{Ψ} are used for the construction of the machining configuration space, as discussed in next section.

4. CONSTRUCTING MACHINING CONFIGURATION SPACE (C-SPACE) AND FINDING THE FEASIBLE REGIONS

In this paper, we are interested in developing a method to optimize 5-axis machining as well as eliminating gouging and global collisions during the tool path planning. Our method works by considering the parameter space for tool orientations and finding the region(s) of orientations that avoid gouging and interference. To do so, a machining *Configuration Space* (C-Space) is constructed for optimizing multi-axis machining, as shown in Figure 5. The earlier mentioned G-buffer model and the cusp height analysis by Equations (5)-(7) are used to construct the machining configuration space. A *Machining Configuration Space* (MCS) of a given CC data CC_i on a part surface *PS* machined with a cutter Ψ is defined as follows:

$$\text{MCS}(\Psi_r, PS, \{CC_i\})_{i=0,...,n} = \begin{bmatrix} \alpha_i \\ \beta_i \\ \delta_i^{\Psi} \end{bmatrix}_{i=0,...,n} \qquad (8)$$

where Ψ_r is the cutter of a radius r used in machining, PS is the part surface, CC_i is the given CC data = $(\mathbf{f}, \mathbf{t}, \mathbf{n}, \mathbf{r}_c)_i$, α_i and β_i are the tilt angle and yaw angle in 5-axis machining, δ_i^{Ψ} is the cusp height at CC_i with tool orientation (α_i, β_i) defined by Equation (7). Figure 5 shows the feasible tool orientation region (α, β) of a cutter contact point CC_i on the part surface *PS*, which satisfies all the machining constraints by eliminating the local/rear gouging and the global collision, as defined by Equation (8).

Since the tool orientation is determined by the (α, β) angle, the tool orientation optimization is to find (α, β) angle such that it not only minimizes the cusp heights but also satisfies the given constraints. In this research, the tool position optimization problem for a given CC_i is formulated as follows:

$$\text{Min.}_{\alpha,\beta}\{\text{Max.}[h_{left}, h_{right}]\} \qquad (9)$$

Subject to: 1) $0° \le \alpha \le 90°$, $-90° \le \beta \le 90°$,
2) no gouging and collision,
3) no joint limit-over.

This is a bi-variable constrained nonlinear optimization problem of non-differentiable functions. To solve this problem efficiently, we investigate the characteristics of 5-axis sculptured surface machining. Some properties of the optimization problem are shown as follows:

Property 1: The lower bound of the objective function is '0'.

If a cusp height has a value less than zero, it means that there is a gouge and this is considered as infeasible in machining.

Property 2: If a tool orientation $(\alpha, \beta)=(0, 0)$ *is feasible, it is optimal.*

Since $\alpha \ge 0$, any cutting ellipses cannot go below the tangent plane at the CC point. This property applies to either convex surface, concave surface or flat surface.

Property 3: The optimal solution lies on the boundary of the feasible region.

Due to the fact that the feasible region is bounded by the machining and geometric constraints of Equation (9), the boundaries of the feasible region are the critical limits when the cutter has been pushed to the extreme orientation without violating these machining and geometric constraints. If an orientation (α, β) for a given CC point is inside the feasible

region, it means that there is room for the cutter to further push between the cutter and the part surface in the vicinity of the CC point. So, the optimal solution always lies on the boundary of the feasible region.

Figure 5 illustrates these properties. To minimize the cusp heights, the cutter has to fit into the surface as closely as possible while it does not gouge or collide with the part surface. Therefore, the optimal orientation (α, β) lies on the boundary of the feasible region. As shown in Figure 5(a), when the surface is planar or convex in the vicinity of a CC point, the orientation (0,0) is optimal if there is no collision or gouging. In Figure 5(b), when the surface is concave shape, the orientation (0,0) is no longer feasible due to local gouging and the optimal solution moves to the boundary of the new feasible region (with the minimum cusp height). In Figure 5(c), if a global collision exists between the cutter and the surface, the feasible tool orientation (α, β) is constrained to a smaller feasible region in the C-Space. Thus the optimal solution changes to the feasible region boundary, as shown in Figure 5(c). Notice that, in Figures 5(b) and 5(c), the searching of the feasible tool orientation moves the original infeasible candidate point (empty circle point in the diagram) to the new feasible point (solid circle point in the diagram), after the machining constraints are added to the C-space. Before these adaptive searches can be conducted in the C-space, the boundaries of the feasible region need to be identified first, which we discuss in the next section.

5. FINDING THE OPTIMAL FEASIBLE TOOL ORIENTAION IN THE C-SPACE

Figure 6 shows the flowchart of finding the optimal feasible tool orientation for the given CC paths. Given a cutter contact point CC_i in the CC paths, the feasible regions of tool orientation (α, β) in the C-Space are first constructed and the local optimal tool orientation is selected. The generated local optimal tool orientations for the CC paths are then processed to find the global optimal tool paths. Two procedures, *forward smoothing* and *backward smoothing*, are conducted to find the global optimal tool orientations by reducing the dramatic changes of tool orientations during 5-axis machining, as shown in Figure 6. Details of the procedures are discussed in this and the next section.

To find the boundary of the feasible region in the C-Space, we developed an algorithm for constructing the C-space feasible region boundaries based on the *edge detection technique* from computer vision. Figure 7 shows the procedure of finding the C-space feasible region boundaries. To speed up the initial searching process, the (α, β) domain is divided into a coarse-grid mesh with a large ($\Delta\alpha$,$\Delta\beta$) interval, as the rectangles shown in Figure 7(a). Once an initial feasible point (α, β) (shown as the double circle in Figure 7(a)) is initially detected by the coarse grid points, the fine-grid mesh with a smaller ($\Delta\alpha$',$\Delta\beta$') is used for detailed checking. In Figure 7(a), the fine grid points are shown as the circular points. The method is to use an edge detection algorithm to start at the initially detected boundary point (the double circle point in Figure 7) and to find the boundary by marching along the feasible region. The edge detection algorithm works as follows (also in Figure 7). As shown in Figure 7, the boundary detection is done by looking forward from the current checking point (α_k, β_k) in the C-space. If (α_k, β_k) is a feasible point, the next candidate point (α_{k+1}, β_{k+1}) is found by making a *right turn* from the current moving direction in the C-space, as shown in Figure 7(b). On the other hand, if the current candidate point is not a feasible point, the next candidate point (α_{k+1}, β_{k+1}) is found by making a *left turn*, as shown in Figure 7(b). By repeating the boundary searching procedure, we can construct the feasible region in the C-space. Detailed algorithm of finding the C-space feasible region boundaries are shown as follows:

Algorithm I. Boundary Search for Feasible Regions in The C-Space

Input: Ψ: Cutter Ψ with radius r,
τ: *acceptable tolerance of machined surface;*
CC_i: i^{th} CC-data;
{CG}: coarse grids {CG} in C-space; and
{FG}: fine grids {FG} in C-space;

Output: $BFR\{(\alpha, \beta, \delta)_t\}_S$: boundary of feasible region $BFR_{t,s}$ *where t=0,…,numbofpoints* and *s=0,…,numbofcontours;*
$LOC_{i,S}$: the local optimal orientation $LOC_{i,S}$ at CC_i for each $BFR(\alpha, \beta, \delta)_{t,s}$ and *s=0,…,numbofcontours*.

1. Initialization:
   Close_Loop ⇐ 0; *s_contour* ⇐ 0; k ⇐ 0; t ⇐ 0;
2. Find the boundaries of all the feasible regions $BFR\{(\alpha,\beta, \delta)_{t=0,\ldots,numbofpoints}\}_{s=0,\ldots, numbofcontours}$:

FOR (Each point CG_k of the given coarse grids *{CG} in C-space*)
{Find the machined error δ^{Ψ}_k of CG_k by using Equations (3)-(7);
IF (($\delta^{\Psi}_k \le \tau$) **AND** (CG_k is **NOT** inside f any existing feasible regions $BFR_{t,s=0,\ldots,s\_contour}$))
{Find the first feasible point $FG_j(\alpha_j,\beta_j)$ of the given fine_grids *{FG}* using CG_k and Equation (7);
Initial_Contour_Point ⇐ $FG_j(\alpha_j,\beta_j)$;
Close_Loop ⇐ 0;
t ⇐ 0;
WHILE(Close_Loop == 0) **DO**
{ Calculate the cusp height δ^{Ψ}_{t+1} of the next fine_grid point FG_{t+1} by Equations (3)-(7);
IF ($\delta^{\Psi}_{t+1} \le \tau$)
{ Save FG_{t+1} as a feasible fine_grids;
t ⇐ t+1;
TURN RIGHT to find the next candidate FG_{t+1};
}
ELSE
{ t ⇐ t+1;
TURN LEFT to find the next candidate FG_{t+1}; }
IF (FG_{t+1} == Initial_Contour_Point)
{Close_Loop ⇐ 1; } /* close the contour loop */
} /* end of while-do */
s_contour ⇐ (*s_contour* + 1);
} /* end of IF-δ^{Ψ}_k */
} /* end of FOR-CG_k */

3. Find the local optimal $LOC_{t,S}$ for the feasible regions $BFR\{(\alpha,\beta,\delta)_{t=0,..,t\_point}\}_{s=0,\ldots,s\_contour}$:

FOR (Each $BFR[(\alpha,\beta,\delta)_t]_{s=0,\ldots,s\_contour}$)
{Find $LOC_{i,S}(\alpha, \beta) \Leftarrow$ Min. $\delta_{t,s}[(BFR(\alpha, \beta, \delta)_{t=0,..,t\_point, s}]$ by using Equation (9); }

4. Return the local optimals and the boundary of feasible region $BFR\{(\alpha,\beta,\delta)_{t=0,..,t\_point}\}_{s=0,\ldots,s\_contour}$:
Return (Boundary_of_feasible_region $BFR[(\alpha, \beta, \delta)_{t\_point}]_{s\_contour}$);
Return (Local_optimal_orientation $LOC(\alpha, \beta)_{i, s=0,\ldots,s\_contour}$);

END.

Figure 7 shows an example of finding the feasible regions in the C-space. The initial feasible point is first found from the coarse grid points, and it is used to launch a detailed search of the boundary of the feasible region. As shown in Figure 7, the searching process moves (#1) from the initial feasible point to the next candidate point that is also a feasible grid point in the C-space. The searching takes a right-turn (#2 move) and the next candidate point is an infeasible point that is outside the feasible region. According to the algorithm, the searching takes a left-turn (move #3), and it finds the next candidate point is still an infeasible point in the space, as shown in Figure 7. The searching takes another left-turn (move #4) and it finds a new feasible point after move#4, and it takes a right-turn (move #5) to continue the searching of the feasible region. The procedure (moves #5 - #9, etc.) continues until the searching returns to the original initial search point, as shown in Figure 7.

6. OPTIMAL TOOL PATH GENERATION BY SMOOTHING TOOL ORIENTATION IN THE C-SPACE

After the feasible tool orientations have been identified for each CC point of the tool paths, problems still exist in multi-axis machining. When the sculptured surfaces are complex, especially for compound surfaces that consist of multiple surface patches, the traditional 5-axis tool path generation methods based on the *cusp height minimization* cause dramatic tool orientation changes during the actual 5-axis machining. A large angle change of tool orientations between two sequence CC points may even overrun the machine tool joint's capacity and cause machine errors during machining.

To eliminate such dramatic change of large angles in 5-axis machining, a method of smoothing tool orientations is developed for 5-axis sculptured surface machining. Given a set of cutter contact paths $\{CC_i\}_{i=0,\ldots,n}$, the correspondent feasible regions $\{BFR_{i,k}\}_{k=0,\ldots,m}$ can be found for CC_i, as discussed in the previous section. After the correspondent feasible regions $\{BFR_{i,k}\}_{k=0,\ldots,m}$ in the C-space have been identified, the tool orientations (α_i, β_i) can be smoothed by the *smallest change of tool orientations* among all the possible feasible regions $\{BFR_{i,k}\}_{k=0,\ldots,m}$ in the C-space. The smallest change of tool orientations can be determined by the *shortest C-distance* between the previous optimal tool orientation $(\alpha_{i-1}^*, \beta_{i-1}^*)$ and the next candidate local optimal tool orientations $(\alpha_{i,k}, \beta_{i,k})_{k=0,\ldots,m}$ of its correspondent feasible regions $\{BFR_{i,k}\}_{k=0,\ldots,m}$. The C-distance between $(\alpha_{i-1}^*, \beta_{i-1}^*)$ and $(\alpha_{i,k}, \beta_{i,k})_{k=0,\ldots,m}$ can be found as follows:

$$C\text{-}distance_i^* \Leftarrow \text{Min.}\{(\sqrt{(\alpha_{i-1}^* - \alpha_{i,k})^2 - (\beta_{i-1}^* - \beta_{i,k})^2})_{k=0,\ldots,m}\}_i,$$

$$\text{for } \forall\ i = 1,\ldots,n \qquad (10)$$

For each CC point CC_i, the smoothed tool orientation (α_i^*, β_i^*) can be found by the following algorithm:

Algorithm_II. Optimal Tool Path Generation by Smoothing Tool Orientations in The C-Space

Input: $\{CC_i\}$: Given cutter contact path $\{CC_i\}$ and $i=0,\ldots,numbofCCpoints$,

$\{BFR_{i,k}\}$: the correspondent feasible regions found by **Algorithm_I** and $k=0,\ldots numbofcontours$;

$\{LOC_{i,k}\}$: the local optimal orientation $LOC_{i,k}$ found by **Algorithm_I** for the given CC_i and the $BFR_{i,k}$, where $k=0,\ldots,numbofcontours$.

Output: $STO\{(\alpha_i^*,\beta_i^*)\}$: The smoothed_tool_orientations $STO\{(\alpha_i^*, \beta_i^*)\}$ for the given CC paths $\{CC_i\}$;

1. Initialization:
   $k \Leftarrow 0$; $C\_distance\_forward \Leftarrow 0$;
   $C\_distance\_backward \Leftarrow 0$;
2. Find the optimized tool orientations by *forward smoothing* based on the shortest *C-distance*:
   $STO\_forward \Leftarrow (\alpha_0^*, \beta_0^*)$;
   FOR (Each CC_i of the given cutter contact path $\{CC_i\}_{i=1,\ldots,n}$)
   {Assign $C\_distance_i^* \Leftarrow$ Large_Distance;
   FOR (Each local_optimal_point $LOC_{i,k}(\alpha_{i,k}, \beta_{i,k}, \delta_{i,k})_{k=0,\ldots,numbofcontours}$ of the given $\{BFR_{i,k}\}$)
   {Find $C\_distance_{i,k} \Leftarrow \sqrt{(\alpha_{i-1}^* - \alpha_{i,k})^2 - (\beta_{i-1}^* - \beta_{i,k})^2}$ by using Equation (10);
   IF ($C\_distance_{i,k} < C\_distance_i^*$)
   THEN {Assign $C\_distance_i^* \Leftarrow C\_distance_{i,k}$;
   Assign $(\alpha_i^*, \beta_i^*) \Leftarrow (\alpha_{i,k}, \beta_{i,k})$; }
   } /* End of FOR- $LOC_{i,k}$ */
   Update $C\_distance\_forward <= C\_distance\_forward + C\_distance_i^*$
   Save (α_i^*, β_i^*) into *STO_forward*;
   } /* End of For-CC_i */
3. Find the optimized tool orientations by *backward smoothing* based on the shortest *C-distance*:
   $STO\_backward \Leftarrow (\alpha_n^*, \beta_n^*)$;
   FOR (Each CC_i of the given cutter contact path $\{CC_i\}_{i=n-1,\ldots,0}$)
   { $C\text{-}distance_i^* \Leftarrow$ Large_Distance;
   FOR (Each local_optimal_point $LOC_{i,k}(\alpha_{i,k}, \beta_{i,k}, \delta_{i,k})_{k=0,\ldots,numbofcontours}$ of the given $\{BFR_{i,k}\}$){
   {Find $C\text{-}distance_{i,k} \Leftarrow \sqrt{(\alpha_{i+1}^* - \alpha_{i,k})^2 - (\beta_{i+1}^* - \beta_{i,k})^2}$ by using Equation (10);
   IF ($C\text{-}distance_{i,k} < C\text{-}distance_i^*$)
   THEN {Assign $C\text{-}distance_i^* \Leftarrow C\text{-}distance_{i,k}$;
   Assign $(\alpha_i^*, \beta_i^*) \Leftarrow (\alpha_{i,k}, \beta_{i,k})$; }
   } /* End of For- $LOC_{i,k}$ */
   Update $C\text{-}distance\_backward <= C\text{-}distance\_backward + C\text{-}distance_i^*$
   Save (α_i^*, β_i^*) into *STO_backward*;
   } /* End of For-CC_i */
4. Find the global optimal tool orientations by both the forward and backward smoothings:
   IF ($C\_didtance\_forward$ < C_distance_backward)
   THEN {**Return** ($STO\_forward\{(\alpha_i^*, \beta_i^*)\})_{i=0,\ldots,n}$ }; }
   ELSE {**Return** ($STO\_backward\{(\alpha_i^*, \beta_i^*)\})_{i=0,\ldots,n}$); }

END.

As shown in Figure 6, both Algorithm_I and Algorithm_II are used for determining the optimal CL paths from the given CC paths $\{CC_i\}$. In the first phase, the boundaries of the feasible C-space regions and the local optimal orientations are identified using Algorithm_I. Then, the global optimal orientations are selected

based on both the forward smoothing and backward smoothing of the local optimal orientations by using Algorithm_II.

7. COMPUTER IMPLEMENTATION AND EXAMPLES

The presented techniques and algorithms have been implemented in a prototype system using C++ programming language on Windows NT personal computers. The input to the system is a polyhedral surface model in STL format. Figure 8 shows some examples of sculptured surface parts and the tool path generation for machining.

Figure 9 shows some examples of the feasible regions in the C-space for the example part surfaces. Figure 9(a) shows a simple concave surface and its feasible C-space region. Due to the nature of concave surfaces, the tool has to be inclined to avoid local and rear gouging, as shown in Figure 9(b), which results in the feasible region excluding the zero or near-zero inclination (α) angles in the C-space. Figure 9(b) illustrates the feasible region (the blue colored region) and the optimal point (the solid circle point in the diagram). Figure 9(c) shows another example surface with global collision. To avoid global collision, the cutter has to be rotated with a certain yaw (β) angle, as shown in Figure 9(d). Notice the feasible region of Figure 9(d) is much smaller than that of Figure 9(b) due to the complex surface geometry of the second example.

Figure 10 shows an example compound surface that consists of four surface patches. The cutter contact (CC) paths are generated by using a set of parallel planes for intersection, and the tool orientations are initially selected based on the cusp height minimization. Figures 10(b) shows the generated CC paths and some example tool motions for machining. The CC paths pass through several different surface patches, as shown in Figure 10(b). For demonstration, the tool path (marked in the middle in Figure 10(b)) that passes through three surface patches is used as an example for tool orientation determination. Notice in Figure 10(b), the cutter changes the tool orientation dramatically at the border between the adjacent surface patches.

Figure 11 shows some examples of searching for the feasible tool orientation in the C-space for continuous tool motions in machining. Figure 11(a) shows the cutter moves along the first surface patch, and the tool orientation (α, β) with the lowest cusp height is found in the C-space. There are two feasible regions in the C-space based on the part geometry and the cutter geometry, as shown in Figure 11(a). Figure 11(b) shows the cutter moves into the intersection region of multiple surface patches. Notice the much smaller feasible region of Figure 11(b) due to the complex surface shape at the current CC point. Figures 11(c) and 11(d) show the cutter moves into a new convex surface patch and its correspondent feasible regions. The computational times for searching the feasible tool orientations in the C-space of the CC points in Figures 11(a)-(d) are 2.554, 1.793, 1.653, and 1.371 seconds respectively on a PC with Pentium III 850MHz and 64Mb SDRAM memory.

Figure 12 shows an example of considering smooth tool motions in selecting alternative tool orientations for machining complex surfaces. Figure 12(a) shows the cutter machining a border CC point with the tool orientation selected by the cusp height minimization method. Figure 12(b) shows an alternative tool orientation at the same CC point as Figure 12(a). As shown in Figure 12(c), there are two feasible regions to machine the CC point, and both Figures 12(a) and 12(b) are locally optimal in the correspondent feasible regions. As shown in Figure 12(c), although the tool orientation found by the traditional local gouging avoidance method has smaller local cusp height (0.26 of Figure 12(a)), the tool orientation of Figure 12(b) should be selected to provide smooth and continuous 5-axis tool motion since it avoids the dramatic change of tool orientations when machining the compound surfaces. Figure 13 shows the tool motions of the example tool path. Figure 13(a) shows the tool motions based only on cusp height minimization, and the tool has several large changes of tool orientations when it moves into the borders of multiple surface patches. Figure 13(b) shows the much smoother tool motions for machining the same example part with the consideration of global smooth tool motions and the smallest orientation changes.

Figure 14 shows the searching for the global optimal orientations of CC paths by both the forward smoothing and backward smoothing methods for the example shown in Figure 13. In Figure 14, the dotted lines in the C-Space represent the forward smoothing of the example CC path of Figure 13(a), and the solid lines show the backward smoothing of the CC path of Figure 13(b). Notice that the dotted lines in Figure 14 show the large change of tool orientation (α, β) between tool orientations 1 and 2 as well as 7 and 8 of the forward smoothing CC path depicted earlier in Figure 13(a). In Figure 14, the total C-distance of the backward smoothing CC path (solid lines) is smaller than that of the forward smoothing CC path (dotted lines). The smaller C-distance of the backward smoothing CC-path is selected as the global optimal tool orientation for 5-axis machining. This is because the backward smoothing CC path (Figure 13(b)) considers the example surface shape change, and in return it results in the smaller orientation changes and smoother tool motions. Figures 13 and 14 show that, by considering the global tool motions and the continuity of tool orientations, the developed method can generate the optimal multi-axis tool motions to maintain smooth and continuous tool motions. This is especially important when the tools are moving at a higher speed and feed rate (for example, high speed machining) in multi-axis sculptured surface machining.

8. Conclusions and Future Research

This paper presents a geometry analysis and C-space searching method to find the optimal tool orientations for 5-axis sculptured surface machining. Techniques of constructing the machining configuration space (C-space) have been developed to determine the feasible tool orientations by considering local gouging, rear gouging, global collisions and machine limits. Both local and global surface geometries are considered in determining tool orientations for machining. To overcome the common weakness of the dramatic change of tool orientations generated by the traditional tool path planning methods, a new method has been developed to smooth the tool motions by searching the alternative tool orientations in the C-space with the smallest change of tool orientations. The techniques presented in this paper exploit the current capabilities of the CAD/CAM systems and the 5-axis machining for better NC tool orientation control. Compared to the traditional user-defined tool orientation in tool path generation and the graphical error verification, the techniques presented in this paper can be used to automatically find the optimal tool orientations adaptive to the complex surface shapes. The method presented in this paper can be used to support the automatic planning and programming of high performance 5-axis sculptured surface machining.

In the future research, the impacts of the minimum cusp heights during the smoothing of tool orientations need to be considered in the 5-axis tool path optimization. To final the global optimal tool orientations for compound surfaces (multiple surface patches) machining, the optimization and smoothing of tool orientations could possibly be conducted in the global machine coordinate system instead of the local coordinate system, i.e., the $(\lambda, \omega)_{global}$ parameter instead of $(\alpha, \beta)_{local}$, with necessary coordinate transformation. The authors are currently looking into these possibilities.

ACKNOWLEDGMENTS

The authors would like to thank the National Science Foundation *CAREER Award* (DMI-9702374) and the Army Research Office (Grant #DAAG55-98-D-0003) to Dr. Y.S. Lee at North Carolina State University. This research was also partially

supported by the Korea Science and Engineering Foundation through the Research Center for Aircraft Part Technology at Gyeongsang National University. Their support is greatly appreciated.

REFERENCES

[Balasub 00] Balasubramaniam M, Laxmiprasad P, Sarma S, Shaikh Z, Generating 5-axis NC roughing paths directly from a tessellated representation, *Computer-Aided Design* 2000;32: 261–277.

[Chiou 99] Chiou CJ, Lee Y-S, A shape-generating approach for multi-axis machining G-buffer models, Computer-Aided Design 1999;31:761–776.

[Chiou 02] Chiou, C.J., and Lee, Y-S., "Machining Potential Field Approach to Tool Path Generation for Multi-Axis Sculptured Surface Machining " *Computer-Aided Design*, Vol. 34, No. 5, 2002, pp. 357-371.

[Cho 93] Cho H.D., Jun Y.T., and Yang M.Y., "Five-axis CNC milling for effective machining of sculptured surfaces," *International Journal of Production Research*, 1993;31(11):2559-2573.

[Choi 93] Choi BK, Park JW, Jun CS. Cutter-location data optimization in 5-axis surface machining, *Computer- Aided Design* 1993;25(6):377-386.

[Choi 98] Choi BK, Jerard RB. *Sculptured Surface Machining*, Dordrecht: Kluwer Academic Publishers, 1998.

[Deng 96] Deng Z, Leu MC, Wang L and Blackmore D, "Determination of Flat-End Cutter Orientation in 5-Axis Machining," *Manufacturing Science and Engineering, ASME*, MED-V4, 1996; 73-80.

[Elber 99]Elber G, Cohen E, "A unified approach to verification in 5-axis freeform milling environments," *Computer-Aided Design*, 1999;31:795–804.

[Jerard 91] Jerard RB, Angleton JM and Drysdale RL, "Sculptured Surface Tool Path Generation with Global Interference Checking," Proceedings of The *ASME Design Productivity International Conference*, Honolulu, Hawaii, February 1991, pp. 737-742.

[Jun 02] Jun CS., K. Cha and Y-S. Lee, "Optimizing Tool Orientations for 5-Axis Machining by Configuration-Space Search Method," Accepted for publication in *Computer-Aided Design*, 2002.

[Kim 94] Kim B.H. and Chu C.N., "Effect of cutter mark on surface roughness and scallop height in sculptured surface machining," *Computer-Aided Design*, 1994;26(3):179-188.

[Kim 95] Kim C.B., Park S. and Yang M.Y., "Verification of NC tool path and manual and automatic editing of NC code," *International Journal of Production Research*, 1995;33(3):659-673.

[Koc 00] Koc B, Ma Y, and Lee Y-S, "Smoothing STL Files by Max-Fit Biarcs Curves for Rapid Prototyping," *Rapid Prototyping Journal*, 2000:6(3):186-203.

[Kruth 99] Kruth JP, Lauwers B, Dejonghe P, Dotremont J, Optimized NC-toolpath generation for 5-axis machining of complex surfaces, *Machining Impossible Shapes* (Olling GJ et. al. ed.), Boston: Kluwer Academic Pub, 1999:343-350.

[Lee 95] Lee Y-S, Chang TC. 2-Phase approach to global tool interference avoidance in 5-axis machining, *Computer-Aided Design*, 1995; 27(10):715-729.

[Lee 97a] Lee Y-S, Admissible tool orientation control of gouging avoidance for 5-axis complex surface machining, *Computer-Aided Design*, 1997; 29(7):507-521.

[Lee 97b]Lee Y-S, Ji H. Surface interrogation and machining strip evaluation for 5-axis CNC die and mold machining, *International Journal of Production Research* 1997;35(1):225-252.

[Lee 98a] Lee Y-S, Non-isoparametric tool path planning by machining strip evaluation for 5-axis sculptured surface machining, *Computer-Aided Design* 1998;30(7):559-570.

[Lee 98b] Lee Y-S, Koc B, Ellipse-offset approach and inclined zig-zag method for multi-axis roughing of ruled surface pockets, *Computer-Aided Design*, 1998;30(12):957–971.

[Li 94] Li SX, Jerard R. 5-axis machining of sculptured surfaces with a flat-end cutter, *Computer-Aided Design*, 1994;26(3):165-178.

[Lo 99] Lo CC, Efficient cutter-path planning for five-axis surface machining with a flat-end cutter, *Computer-Aided Design* 1999;31:557–566.

[Marciniak 87] Marciniak K. Influence of surface shape on admissible tool positions in 5-axis face milling. *Computer-Aided Design* 1987;19(5):233–6.

[Morishige 99] Morishige K, Nasu T, Takeuchi Y. Five-axis control sculptured surface machining using conicoid end mill, *Machining Impossible Shapes* (Olling GJ et. al. ed.), Boston: Kluwer Academic Publishers, 1999:366-375.

[Ray 92] C.Ray, *Robots and manufacturing automation*, John wiley & Sons, 1992.

[Rao 00] Rao A, Sarma R, On local gouging in five-axis sculptured surface machining using flat-end tools, *Computer-Aided Design*, 2000;32:409-420.

[Suresh 94] Suresh K, Yang DCH, Constant scallop-height machining of free-form surfaces, *Journal of Engineering for Industry*, 1994;116(2):253-259.

[Vickers 89] Vickers GW, Ly MH, Oetter RG, *Numerically controlled machine tools*, Ellis Horwood, New York, 1990. +

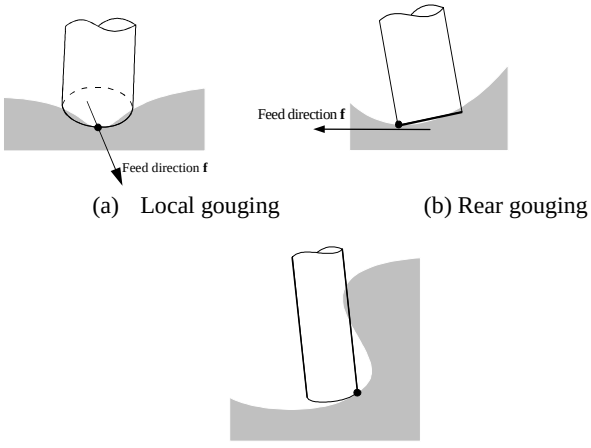

(a) Local gouging (b) Rear gouging

(c) Global collision

Figure 1. Different types of gouging and interferences in 5-axis machining

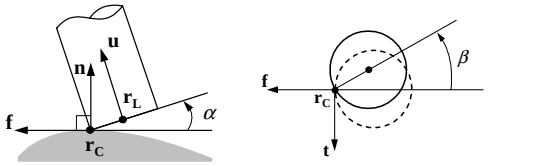

(a) Tilt angle α (b) Yaw angle β

Figure 2. Tilt angle and yaw angle in 5-axis machining

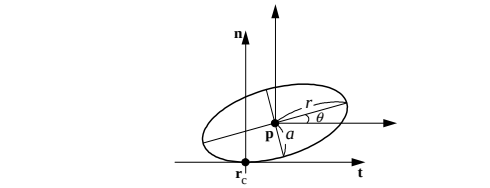

(a) Cutting ellipse in 5-axis machining

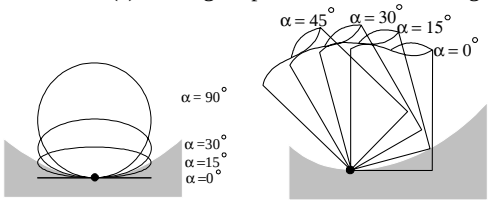

(b) Effects of the tilt angle

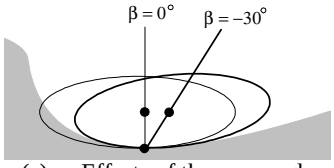

(c) Effects of the yaw angle

Figure 3. Changes of the tilt and yaw angles to avoid local and rear gouging

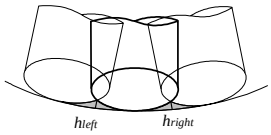

(a) Exact cusp height

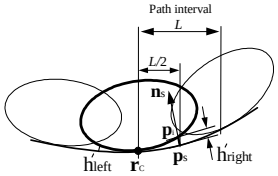

(b) Cusp height *h* between the adjacent tool paths

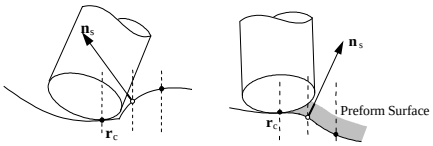

(c) Surface normal and the machined surface errors

Figure 4. Machined surface error analysis by the cutting ellipse shapes and G-map methods

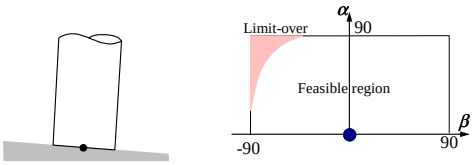

(a) A tool on a planar surface and its feasible region

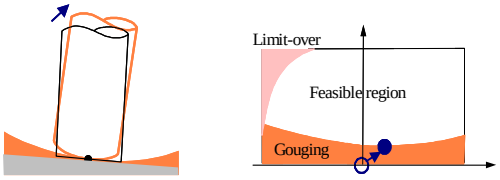

(b) Local gouging avoidance and the feasible configuration space

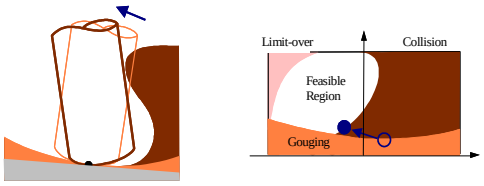

(c) Global collision avoidance and the feasible region in the machining configuration space

Figure 5. The feasible machining configuration space

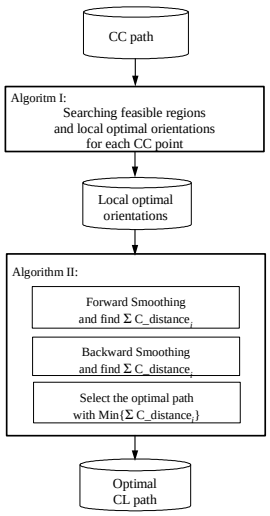

Figure 6. Overall procedure in the machining configuration space for the optimal tool orientation

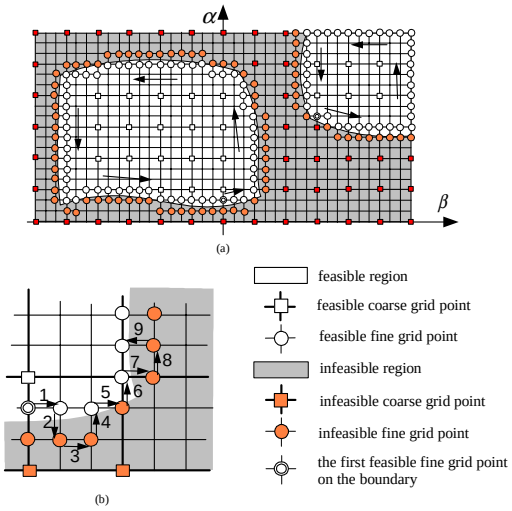

Figure 7. Boundary search in the configuration space by using the edge detection algorithm

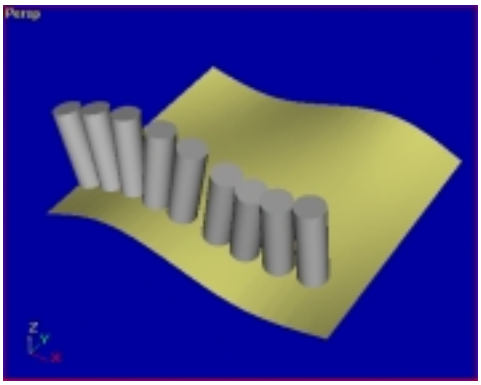

(a)

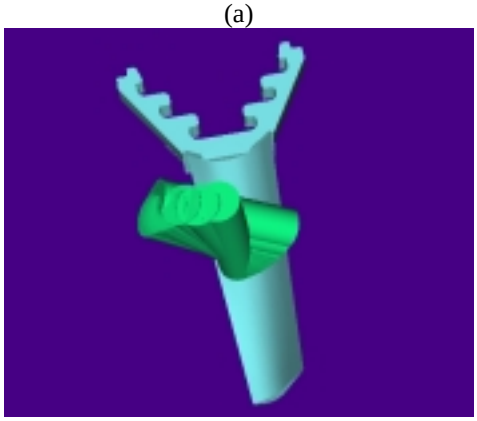

(b)

Figure 8. Examples of tool paths for sculptured surface machining (a) Tool path generation for machining a surface, (b) Machining of an example turbine blade

(a) (b) Optimal tool orientation in C-space without gouging

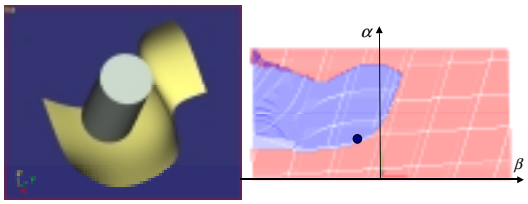

(c) Avoiding global collision in machining (d) Optimal tool orientation in C-space without global collision

Figure 9. Example of the feasible regions and optimal orientations in the configuration space (C-space) by eliminating the local gouging and the global collision

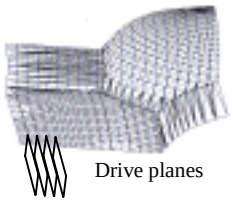

(a) An example of compound sculptured surface and CC path generation

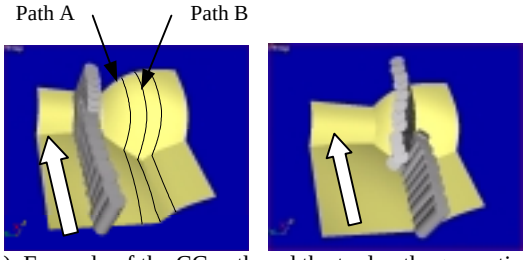

(b) Example of the CC path and the tool path generation

Figure 10. Example of a compound sculptured surface and the tool path generation

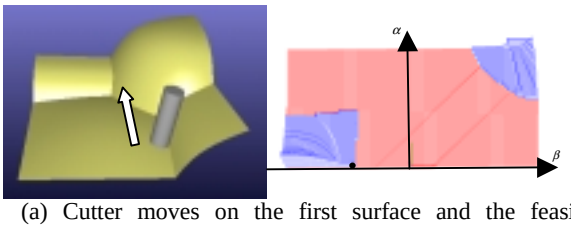

(a) Cutter moves on the first surface and the feasible tool orientation in the (α, β) configuration space

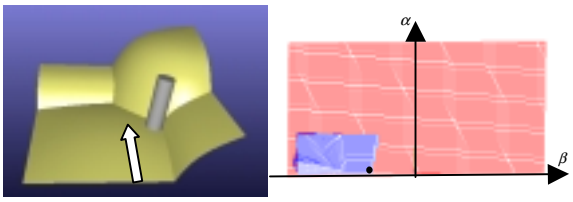

(b) Cutter moves into the region where multiple surfaces meet

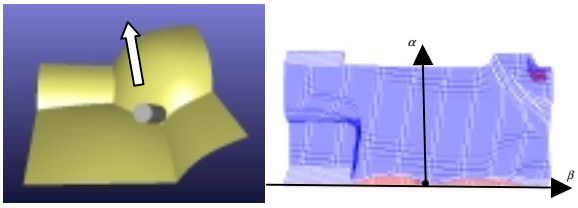

(c) Cutter moves onto the second surface and the feasible region in the (α, β) C-space

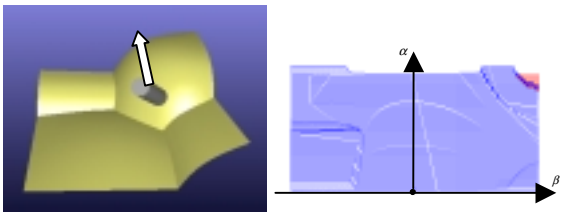

(d) Cutter continues to move on the second surface

Figure 11. Searching the feasible configuration space and generating the continuous tool path along Path B (see Fig. 14)

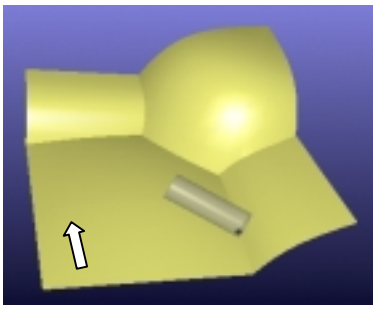

(a) Local optimal tool orientation (by cusp height minimization)

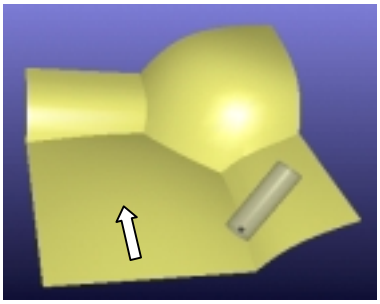

(b) Alternative tool orientation

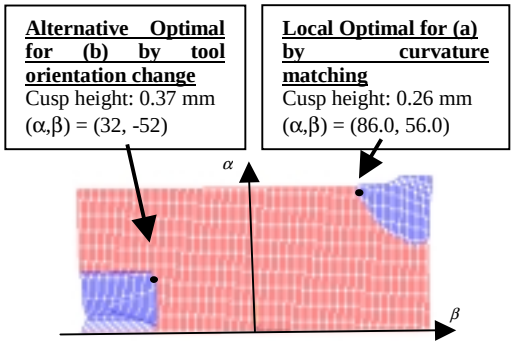

(c) Smoothing tool orientation change by considering continuous tool motions

Figure 12. Global optimization of tool path by backward smoothing the tool orientation changes in machining

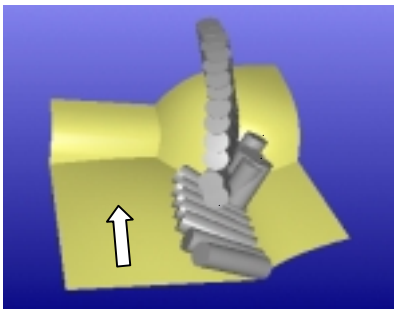

(a) Locally optimized tool paths (surface curvature fitting) for machining the example surfaces

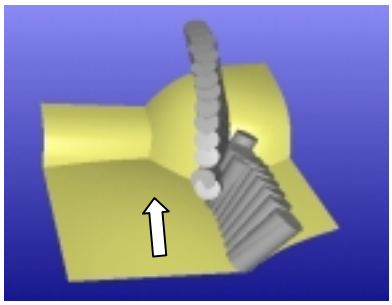

(b) Globally optimized tool paths by smoothing tool orientation change for compound surface machining

Figure 13. Global optimization and smoothing of continuous tool orientation control for 5-axis sculptured surface machining

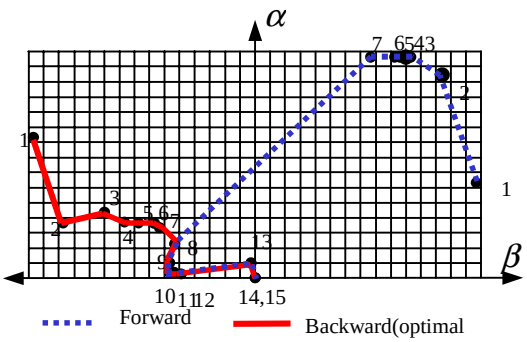

Figure 14. Finding the global optimal tool path with the minimal tool orientation change by both the forward smoothing and the backward smoothing